

Nasal absorption and biodistribution of plasmid DNA: an alternative route of DNA vaccine delivery

Yu-Kyoung Oh ^{a,*}, Jong-Pil Kim ^a, Tae Sun Hwang ^b, Jung Jae Ko ^a, Jung Mogg Kim ^c,
Ji-Sun Yang ^d, Chong-Kook Kim ^e

^a Department of Microbiology and Institute of Medical Research, College of Medicine, Pochon CHA University, Kyonggi-do 487-800, South Korea

^b Department of Anatomy, College of Medicine, Pochon CHA University, Kyonggi-do 487-800, South Korea

^c Department of Microbiology and Institute of Biomedical Science, College of Medicine, Hanyang University, Seoul, South Korea

^d Department of Pharmacology, Korea Food and Drug Administration, Seoul, South Korea

^e College of Pharmacy, Seoul National University, Seoul, South Korea

Received 1 February 2001; received in revised form 9 May 2001; accepted 9 May 2001

Abstract

Nasal administration is emerging as a new route of DNA vaccine delivery. We aimed to study the extent of absorption and biodistribution of intranasally administered plasmid DNA. After intranasal administration, the level of plasmid DNA in the serum peaked at 1.5 h. The ratio of the area under the concentration (AUC) after intranasal administration of DNA over the AUC after intravenous administration was 0.14. At 15 min post inoculation, the highest organ distribution was observed in the liver and the cervical lymph nodes showed the highest level among the lymph nodes. At 24 h a higher localization of plasmids to the brain than to the lung and spleen was notable. A significant level of mRNA expression was observed in the lymph nodes. These results suggest that plasmid DNA can be substantially absorbed and distributed to the lymph nodes after intranasal administration, partly explaining the systemic immunogenicity of intranasally administered plasmid DNA vaccines. © 2001 Elsevier Science Ltd. All rights reserved.

Keywords: Plasmid DNA; Nasal absorption; Distribution

1. Introduction

Recently, intranasal routes of DNA administration have been drawing attention in genetic vaccines and other gene therapy fields. Nasal immunization of mice with human papillomavirus-16 L1 gene was shown to induce cytotoxic T lymphocytes in vaginal draining lymph nodes [1]. Intranasal administration of *Cryptosporidium parvum* DNA was reported to induce systemic and intestinal immune responses [2]. Kuklin et al. [3] demonstrated that the direct nasal gene transfer of immunomodulatory cytokines such as TGF- β could provide a convenient means of modulating immunity. Moreover, the nasal route is emerging as a new route of

administering therapeutic genes for treatment of cystic fibrosis [4].

However, these studies have mainly reported the immunity and therapeutic outcomes of intranasally administered genes. Despite that the efficacy by which intranasally administered plasmid DNA is absorbed and reaches the organs in the body would be important to design more effective gene therapy or nasal genetic vaccines, little is understood regarding the extent of absorption and the fate of intranasally administered plasmid DNA.

Here, we studied the efficacy of absorption and body distribution of intranasally administered plasmids using a quantitative polymerase chain reaction (PCR)-based assay. We report the absorption kinetics and extents of intranasally administered plasmid DNA, and its significant distribution to the lymph nodes and various organs.

* Corresponding author. Tel.: +82-31-542-6671; fax: +82-31-543-2818.

E-mail address: ohyk@hotmail.com (Y.-K. Oh).

2. Materials and methods

2.1. Animals

Female BALB/c mice were purchased from Charles River Japan (Atsugi, Japan). The mice were used at 6–8 weeks of age. Animals received food and water ad libitum.

2.2. Plasmid DNA preparation

As a model plasmid, pCMV β (Clontech, Palo Alto, CA, USA) encoding the gene for β -galactosidase was used. The plasmid DNA was amplified using *Escherichia coli* DH5 α and purified using the Qiagen Giga Prep kit (Qiagen, Santa Clarina, CA, USA). The purity of DNA preparations was confirmed on a 1% agarose gel. All plasmid preparations were found to contain fewer than three endotoxin units per mg of purified DNA by the limulus amebocyte lysate assay (Sigma, St. Louis, MO, USA).

2.3. Construction of the competitor

The competitor used as an internal standard of quantitative PCR was the 188 bp deleted mutant of pCMV β , named as pdmCMV β . The construction scheme of the competitor is shown in Fig. 1. Target plasmids were digested with Xho I and Sma I which generated two fragments sized 188 bp and 6976 bp. The linearized plasmid of 6.97 Kb size was gel purified on a 1% agarose gel. Next, the Xho I site of the linearized plasmid was blunt-ended with the Klenow fragment, and religated to the other blunt end of Sma I. The ligation mixture was transformed into competent *E. coli* DH5 α cells and ampicillin-resistant colonies obtained were analyzed by PCR. The product obtained by PCR was 261 bp as compared to 449 bp of the wild type. The sense primer was 5'-TTGACCTCCATAGAAGACAC-CGG-3' and the antisense primer was 5'-CCCAACT-

TAATCGCCTTGCAG-3'. The lack of Xho I and Sma I sites in the competitor was confirmed by restriction endonuclease digestion.

2.4. Competitive and quantitative PCR-based assay

Competitive PCR was performed by adding various amounts of the competitor plasmids to the reaction mixtures containing the same amount of sample DNA. Sense and antisense primers described above were used for amplification of 449 bp and 261 bp fragments from pCMV β and pdmCMV β , respectively. PCR was performed in a 0.2 ml reaction tube containing 50 μ l of PCR mixture composed of 1 μ l sample DNA, 1 μ l of the competitor plasmid, 4 μ l 2.5 mM dNTPs, 5 μ l 10X reaction buffer (50 mM Tris pH 8.0, 100 mM NaCl, 0.1 mM EDTA, 1 mM dithiothreitol, 50% glycerol and 1% Triton X-100), 10 pmole of each primer, and 1 U Taq polymerase. The mixture was cycled in a Perkin–Elmer model 2400 thermocycler at 94 °C for 30 s, 57 °C for 30 s, and 72 °C for 30 s for the appropriate number of cycles.

Subsequently, the amplicons of each reaction were split on a 2% agarose gel. A comparison of the PCR products was then used to determine the quantity of the target plasmid DNA in the samples. The density of each band was measured using a gel-doc image analyzer (Vilber Lourmat, France). In each competitive PCR run, an internal standard curve was obtained by plotting the log values of target/competitor density ratios against the log amounts of the competitor initially added to the reaction. The quantitation was made graphically. The amount of target DNA in the samples was read from the x -axis intercept where the log ratio of target/competitor density became zero. Samples exceeding the calibration curve were diluted in TE buffer before repeated analysis.

2.5. Administration of plasmid DNA

Before the intranasal administration of plasmids, animals were anesthetized with a single intraperitoneal dose of ketamine hydrochloride (80 μ g/g). Plasmids were administered into the nostrils using a micropipette. Each mouse received a total of 50 μ g of plasmid DNA in 20 μ l of phosphate-buffered saline per administration. In some cases, plasmids (50 μ g) were intravenously injected into the tail vein of the mouse.

2.6. Preparation of biological samples

At various time points after administration, approximately 30 μ l of blood was collected from the tail vein using a capillary tube with 1.1 mm diameter. Total DNA of serum was extracted according to a method described by Zerbini et al. [5] but slightly modified. In

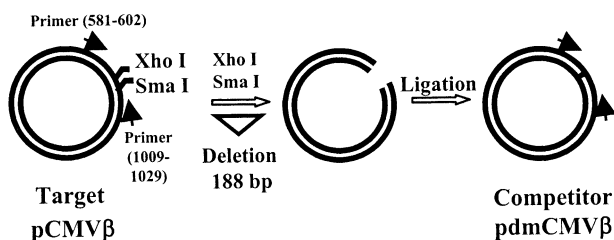


Fig. 1. Diagram of the procedure for cloning of the internal standard competitor plasmid DNA with 188 bp deletions. After digesting target plasmids with Xho I and Sma I, the linearized plasmid of 6.97 kb size was gel purified. The Xho I site of the linearized plasmid was blunt-ended, and religated to the other blunt end of Sma I. The ligation mixture was transformed into competent *E. coli* DH5 α cells and screened by PCR.

brief, serum samples were heated at 90 °C for 3 min to inactivate nucleases and centrifuged at 15,000 g for 1 min to precipitate proteins. The supernatant was directly used in the competitive PCR.

For biodistribution study mice were sacrificed at 15 min and 24 h post dose. Organs, nasal tissues, muscles and lymph nodes were harvested. To minimize the influence of plasmid DNA in blood circulating through the tissues at the time of sampling, the samples were thoroughly washed several times with saline, blotted dry, and weighed. The samples were then suspended into DNAzol® (Gibco BRL, NY, USA) with a concentration of 50 mg tissue per ml, and homogenized using Teflon tissue grinders. The tissue grinders were changed after each tissue homogenation to avoid cross-contamination of the tissues. The homogenates (500 µl) were then loaded onto Wizard® DNA clean up column (Promega, WI, USA). After washing steps, the DNA was eluted with 50 µl of TE buffer.

2.7. Pharmacokinetic assessments

Pharmacokinetic data were analyzed by the noncompartmental method. The area under the curve (AUC) was estimated over 24 h using the linear trapezoidal integration method. The extent of absorption of intranasally administered plasmid DNA was determined by the ratio of AUC_{in} (AUC after intranasal administration) over AUC_{iv} (AUC after intravenous administration) times 100.

2.8. Reverse transcription PCR (RT-PCR) analysis

To determine the mRNA expression of administered plasmid DNA in the lymph nodes, the mice were sacrificed at 24 h after intranasal administration of plasmid DNA (50 µg/mouse), and the lymph nodes were removed. Total RNA was extracted from each lymph node using a TRIzol® reagent (Gibco BRL, NY). The cDNA was prepared using a First-Strand cDNA synthesis kit (Boehringer Mannheim, IN). PCR amplification of the 1036 bp segment of the β-galactosidase gene was performed using primers as described previously [6]. A primer pair to amplify a 360 bp segment of GAPDH gene was 5'-ATCACCATCTTCCAGGAGC-3' for the sense and 5'-AGAGGGGCCATCCACAGTCTTC-3' for the antisense. PCR products were analyzed by electrophoresis on 2% agarose gel.

2.9. Statistics

Statistical analysis of data was performed using Student's T-test or analysis of variance (ANOVA). A *p* value of less than 0.05 was considered significant.

3. Results

3.1. Quantitative PCR-based assay of pCMVβ

For the assay of plasmid DNAs in biological samples, a sensitive and quantitative PCR strategy was employed. Quantitative PCR is based on coamplification of the sample template together with various amounts of the internal standard molecule (competitor) sharing with the target the primer recognition sites, but differing in size. pCMVβ, widely used to test various gene delivery systems, was chosen as a target plasmid. As illustrated in Fig. 1, the competitor was constructed to share the same sense and antisense primer used for target amplification. The expected PCR product was 449 bp and 261 bp for the target and the competitor, respectively.

The primers used in this study were specific for pCMVβ. When PCR was run after spiking of pCMVβ to the serum or DNA extracts of tissues, no size variants in PCR products on agarose gel were observed up to 30 cycles. However, from 32 cycles an extra band was observed (data not shown) probably due to the formation of heteroduplex. Accordingly, 30 cycles were chosen for subsequent PCR reaction. Moreover, to test the possibility of cross-contamination in PCR, we processed and ran the samples of untreated animals as a negative control. However, no PCR product was observed in the negative control, indicating that PCR positivity in samples was not due to cross-contamination (data not shown).

The coamplification of the target with various amounts of the competitor generated PCR products of relatively different band densities (Fig. 2A). The quantitation of PCR products by densitometry resulted in a calibration curve showing a linear relationship over an extended range of DNA concentrations. An example of the internal standard curve is shown in Fig. 2B. The curve also shows that as low as fg-level plasmids were detectable by quantitative PCR. The amount of pCMVβ in the biological samples was similarly calculated from the internal standard curve based on the ratio between PCR product originating from the sample and the corresponding internal standard competitor. The internal standard curve was obtained at each run.

3.2. Kinetics and extent of plasmid DNA absorption after intranasal administration

Using quantitative PCR, the absorption of intranasally administered plasmids was studied. Following intranasal administration, detectable amounts of plasmids were absorbed into the systemic circulation showing 150 ± 83 pg/ml of serum concentration at 5 min (Fig. 3A). The maximum serum concentration (C_{\max}) was 430 ± 86 pg/ml, reached at 90 min postdose.

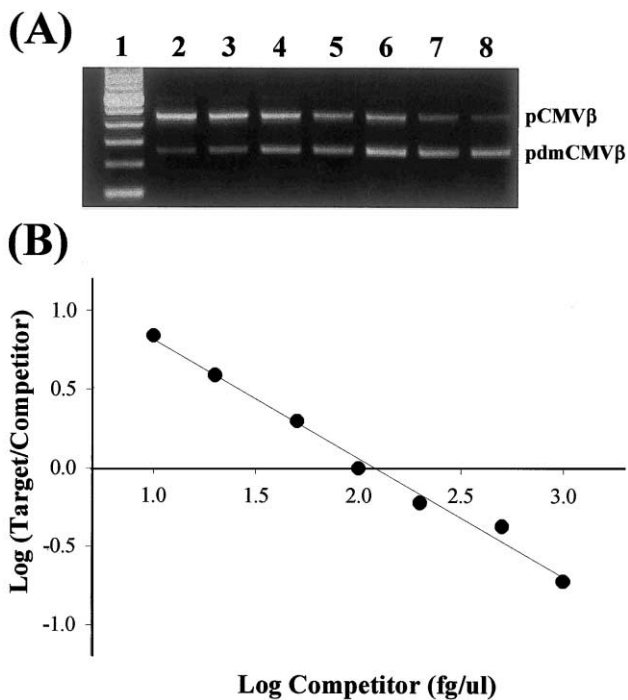


Fig. 2. Quantitative PCR relative to pCMV β . (A) The amounts of competitor for PCMV β were 10 fg/ μ l (lane 2), 20 fg/ μ l (lane 3), 50 fg/ μ l (lane 4), 100 fg/ μ l (lane 5), 200 fg/ μ l (lane 6), 500 fg/ μ l (lane 7), 1000 fg/ μ l (lane 8). Lane 1, 1 kb size marker. The constant amount of the target plasmid DNA was present in all the samples. (B) The ratio between the intensities of the bands at each lane was plotted against the amount of internal standard added. $r^2 = 0.994$.

The value of AUC_{in} was $1.5 \times 10^3 \pm 0.62 \times 10^3$ pg h/ml. After intravenous administration, the serum levels of plasmid DNA showed rapid declination until 20 min, followed by a slower elimination phase (Fig. 3B). The value of AUC_{iv} was $11 \times 10^3 \pm 2.8 \times 10^3$ pg h/ml. The extent of intranasal absorption, defined by the ratio of AUC_{in}/AUC_{iv} $\times 100$, was 14%.

3.3. Biodistribution of intranasally administered plasmid DNA

The biodistribution of plasmids was measured at 15 min and 24 h postdose. At 15 min after intranasal administration, the organ distribution of plasmids was the highest in the liver, followed by the kidney, heart, lung, brain and spleen (Fig. 4). At 24 h postdose, the highest distribution was also found in the liver. Notably, the distribution of plasmids to the brain was comparable to that to the lung at 15 min post inoculation. At 24 h, the level of plasmid DNA in the brain was 3.9- and 4.8-fold higher than that in the lung and the spleen, respectively (Fig. 4).

The level of plasmids was as high as 7.4×10^5 pg/mg at the nasal tissues at 15 min after administration, but rapidly declined showing only 1.4 pg/mg at 24 h post inoculation (Fig. 5). Similar to nasal tissues, muscle

tissues showed a substantial declination in the levels of plasmids at 24 h post inoculation.

To test whether the systemically absorbed plasmid DNA could distribute to the tissues of the immune system, the levels of DNA in various lymph nodes were determined. Of lymph nodes, the draining cervical lymph nodes showed more than a six-fold higher level of plasmids (960 ± 350 pg/mg) than other lymph nodes, such as mesenteric and iliac lymph nodes, at 15 min post inoculation (Fig. 5). However, at 24 h the level of plasmid DNA in the cervical lymph nodes was greatly reduced, showing 0.47 ± 0.2 pg/mg. There was no significant difference in the level of plasmids among the lymph nodes at the time point (ANOVA, $p > 0.05$).

Given the significant distribution of plasmid DNA to the lymph nodes, we further tested the expression of DNA delivered to the lymph nodes. The RT-PCR data (Fig. 6) display that plasmid DNA could be expressed at the various lymph nodes, including the cervical, mesenteric, and iliac lymph nodes. GAPDH was used as an endogenous reference.

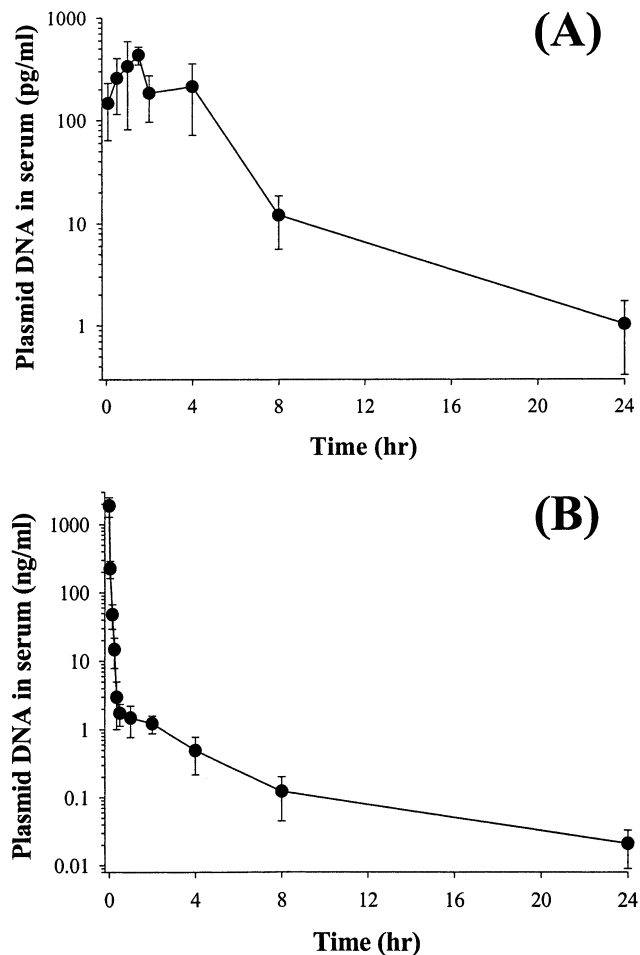


Fig. 3. Serum concentration–time profiles of plasmid DNA. Plasmid DNA (50 μ g) was administered into a mouse by the intranasal (A) or intravenous (B) route. The amounts of plasmids in the serum were measured by quantitative PCR. The results are expressed as the mean \pm SE ($n = 7$).

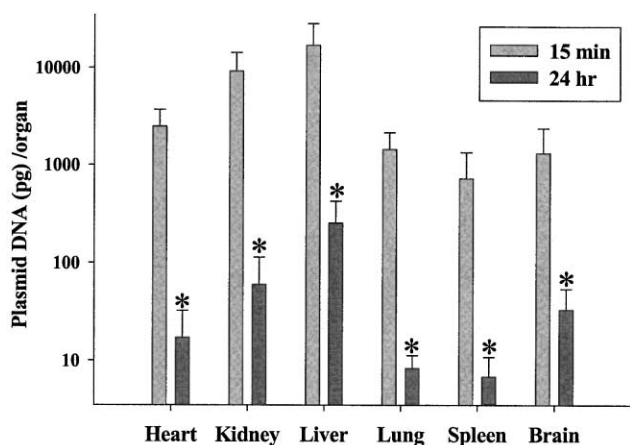


Fig. 4. Organ distribution of intranasally administered plasmid DNA. The distribution of plasmids in the organs at 15 min and 24 h post inoculation was measured by quantitative PCR. The results are expressed as the mean \pm SE ($n = 6$). *: significantly different from the values at 15 min (T-test, $p < 0.05$).

4. Discussion

In this study, we demonstrated that nasally administered plasmid DNA could be substantially absorbed into systemic circulation and distributed to different tissues of the body, including the brain and the lymph nodes.

The competitive and quantitative PCR enabled us to follow the pharmacokinetics of plasmids from the same animal, rather than sacrificing the animals at each experimental time point. Until now, the levels of systemically administered plasmids in the biological sam-

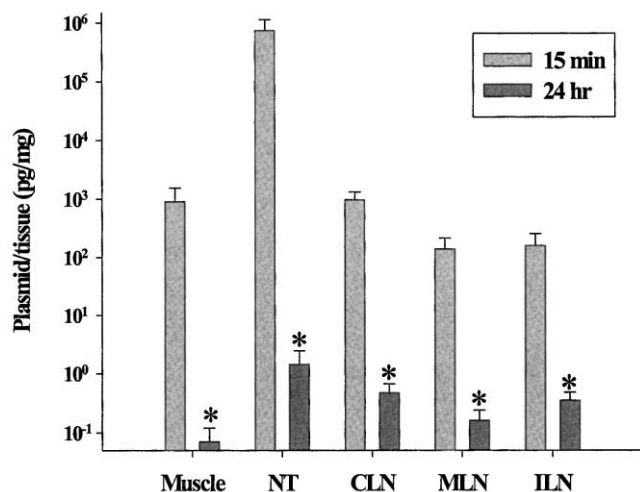


Fig. 5. Biodistribution of intranasally administered plasmid DNA to lymph nodes and tissues. The distribution of plasmids to the lymph nodes and other tissues at 15 min and 24 h post inoculation was measured by quantitative PCR. NT, nasal tissues; CLN, cervical lymph nodes; MLN, mesenteric lymph nodes; ILN, iliac lymph nodes. The results are expressed as the mean \pm SE ($n = 6$). *: significantly different from the values at 15 min (T-test, $p < 0.05$).

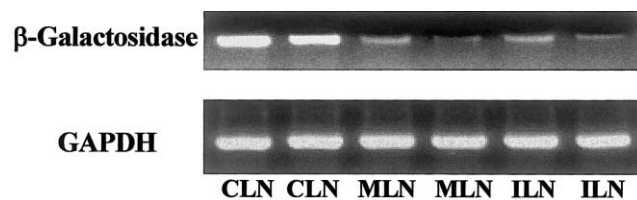


Fig. 6. RT-PCR analysis of β -galactosidase mRNA at the lymph nodes. At 24 h after intranasal administration of plasmid DNA, the mice were sacrificed and the lymph nodes were removed. Total RNA was extracted from each organ using a TRIzol[®] reagent. The cDNA was prepared using a First-Strand cDNA synthesis kit. PCR amplification yielded the 1036 bp segment of the β -galactosidase cDNA and the 360 bp-long GAPDH gene. CLN, cervical lymph nodes; MLN, mesenteric lymph nodes; ILN, iliac lymph nodes. The results are presented in duplicate.

ples have been mostly measured by radiolabelled plasmids [7,8]. However, due to the relatively low sensitivity of the radionuclide approach, whole animals were sacrificed at each time point for sampling ml-level bloods. In this study, thanks to the PCR technique sensitive enough to detect the fg/ μ l level of plasmids in the samples, we only sampled a 30 μ l volume of blood from the same animal at each time point. The competitive PCR utilizing such minute volumes of blood per sampling would be also advantageous in that the total blood volume of a mouse may not be significantly altered after repeated sampling. However, similar to the radionuclide approach where the radioactive parent drugs and metabolites can be indiscriminately detected, one caveat of competitive PCR would be that the whole plasmid DNA might be partially fragmented, degraded, or bound to other molecules in the biological samples even if the PCR region studied is intact. To predict the intactness of the transcription region, the better primers for this kind of study would be the ones that span the promoter to the poly A signal.

The absorption rate of the large molecule pCMV β (7.2 kb) after intranasal dosing appears to be relatively slow compared with other intranasally administered small molecules such as alniditan, dihydroergotamine and sumatriptan, used for treatment of acute migraine. The time to reach C_{max} (T_{max}), used as an index of the speed of absorption, was longer in the intranasally administered pCMV β (90 min) than nasal alniditan (11 min) [9] and dihydroergotamine (54 min) [10], but comparable to sumatriptan (90 min) [11].

The extent of intranasal plasmid DNA absorption (14%) was similar to that of azetirelin (17%), a thyrotropin-releasing hormone analog [12], and higher relative to tetracosactide peptide drug, an adrenocorticotrophic hormone analog (4%) [13]. The mechanism by which large molecule plasmid DNA is substantially absorbed remains to be further investigated. However, the possibility exists that plasmid DNA might interact with the nasal epithelial mem-

branes and transiently affect the tight junctions [14]. Alternatively, there might be a transport system which facilitates the absorption of plasmid DNA across the nasal mucosa.

We found that nasally administered plasmid DNA showed the highest organ distribution in the liver. Similarly, intravenously administered plasmid DNA showed the highest organ distribution in the liver [7]. Such high distribution of nasally administered plasmids to the liver seems to have resulted from the highly phagocytic activities of the reticuloendothelial system mainly present in the liver [15].

The localization of plasmid to the brain appears to be higher after intranasal administration as compared to intravenous administration. It was reported that the distribution of plasmids to the brain was about 145-fold lower than that to the liver at 20 min after intravenous injection of DNA [7]. We observed that the level of plasmid DNA localized to the brain was only 15-fold lower in comparison with the liver at 15 min post inoculation. The higher distribution of plasmids to the brain after intranasal administration indicates that nasal administration might be a potential route for the delivery of therapeutic genes to the brain with reduced side effects to other organs.

Currently, the mechanism by which intranasally administered plasmid DNA showed the higher distribution to the brain is not clear. Previously, the brain distribution of compounds such as an antiparkinsonian drug L-dopa [16], wheat germ agglutinin–horseradish peroxidase [17], and certain viruses [18] were reported to be higher after intranasal delivery than intravenous administration. It has been thought that the intranasally administered materials might be delivered to the brain via the olfactory epithelium route [18]. Thus, we cannot exclude the possibility that intranasally administered plasmids could be directly transported to the brain via the olfactory epithelium.

The rapid declination of plasmid DNA in nasal tissues (Fig. 5) suggests the possibility of rapid mucociliary clearance of plasmid DNA. In addition, the local degradation of plasmids at the mucosal surface appears to be feasible. Such rapid declination in nasal tissues indicates the need for the development of a nasal DNA vaccine delivery system that may prolong the nasal retention of plasmid DNA after administration.

Notably, the muscle showed high accumulation of DNA at 15 min. Currently, it remains unclear by which mechanisms intranasally administered plasmid DNA could be rapidly distributed to the muscle. Although further research definitely needs to be done to pursue the exact mechanisms, one feasibility is that the muscle might offer a sink condition thanks to its large weight portion in the body, allowing high concentration gradients to be maintained between the muscle and other parts of the body. Another possibility is that there

might be an alternative transport pathway of plasmid DNA to the muscle after intranasal administration.

The higher levels of plasmids in cervical lymph nodes observed at 15 min (Fig. 5) may represent the uptake of plasmids by the cellular component of the draining lymph nodes, particularly macrophages, as well as the drainage of plasmids into the lymph nodes. Similar to our results, the higher distribution of the intranasally administered materials in the cervical lymph nodes was observed in the peptide analogs of myelin basic protein [19]. The distribution of plasmids to the lymph nodes implies that intranasally administered DNA vaccines might be well presented to the immune cells, such as macrophages and B cells. Moreover, the mRNA expression of DNA in the lymph nodes (Fig. 6) supports that the intranasally administered plasmid DNA could be delivered to the lymph nodes as a form intact enough to be transcribed.

In conclusion, our results support that an intranasal route providing the substantial absorption of DNA might have potential as a promising non-invasive delivery route of DNA vaccines and other therapeutic genes, although the possible problem of spill over to various tissues such as liver and brain should not be neglected. Moreover, the significant distribution and expression in the various lymph nodes indicate that intranasally administered DNA might be a legitimate route for inducing systemic responses.

Acknowledgements

This work was supported by a grant of the Korea Health 98 R & D Project, Ministry of Health and Welfare, Republic of Korea (HMP-98-D-5-0048).

References

- [1] Dupuy C, Buzoni-Gatel D, Touze A, Bout D, Coursaget P. Nasal immunization of mice with human papillomavirus type 16 (HPV-16) virus-like particles or with the HPV-16 L1 gene elicits specific cytotoxic T lymphocytes in vaginal draining lymph nodes. *J Virol* 1999;73:9063–71.
- [2] Sagodira S, Iochmann S, Mevelec MN, Dimmer-Poisson I, Bout D. Nasal immunization of mice with *Cryptosporidium parvum* DNA induces systemic and intestinal immune responses. *Parasit Immunol* 1999;21:507–16.
- [3] Kuklin NA, Daheshia M, Chun S, Rouse BT. Immunomodulation by mucosal gene transfer using TGF-beta DNA. *J Clin Invest* 1998;102:438–44.
- [4] Graham SM, Launspach JL. Utility of the nasal model in gene transfer studies in cystic fibrosis. *Rhinol* 1997;35:149–53.
- [5] Zerbini M, Gallinella G, Manaresi E, Musiani M, Gentilomi G, Venturoli S. Standardization of a PCR-ELISA in serum samples. *J Med Virol* 1999;59:239–44.
- [6] Oral HB, Larkin DF, Fehervari Z, Byrnes AP, Rankin AM, Haskard DO, Wood MJ, Dallman MJ, George AJ. Ex vivo adenovirus-mediated gene transfer and immunomodulatory protein production in human cornea. *Gene Ther* 1997;4:639–47.

- [7] Nishikawa M, Takemura S, Kadakura Y, Hashida M. Targeted delivery of plasmid DNA to hepatocytes in vivo: optimization of the pharmacokinetics of plasmid DNA/galactosylated poly(L-lysine) complexes by controlling their physicochemical properties. *J Pharm Exp Ther* 1998;287:408–15.
- [8] Kawabata K, Takakura Y, Hashida M. The fate of plasmid DNA after intravenous injection in mice: involvement of scavenger receptors in its hepatic uptake. *Pharm Res* 1995;12:825–30.
- [9] Roon KI, Soons PA, Uitendaal MP, Beukelaar F, Ferrari MD. Pharmacokinetic profile of alniditan nasal spray during and outside migraine attacks. *Br J Clin Pharmacol* 1999;47:285–90.
- [10] Humbert H, Cabiac MD, Dubray C, Lavene D. Human pharmacokinetics of dihydroergotamine administered by nasal spray. *Clin Pharmacol Ther* 1996;60:265–75.
- [11] Moore KHP, Hussey EK, Fuseau E, Duquesnoy C, Pakes GE. Safety, tolerability, and pharmacokinetics of sumatriptan in healthy subjects following ascending single intranasal doses and multiple intranasal doses. *Cephalalgia* 1997;17:541–50.
- [12] Kagatani S, Inaba N, Fukui M, Sonobe T. Nasal absorption kinetic behavior of azetirelin and its enhancement by acycarnitines in rats. *Pharm Res* 1998;15:77–81.
- [13] Wuthrich P, Martenet M, Buri P. Effect of formulation additives upon the intranasal bioavailability of a peptide drug: tetracosactide. *Pharm Res* 1994;11:278–82.
- [14] Marttin E, Verhoef JC, Merkus FW. Efficacy, safety and mechanism of cyclodextrin as absorption enhancers in nasal delivery of peptide and protein drugs. *J Drug Target* 1998;6:17–36.
- [15] Hussain AA. Intranasal drug delivery. *Adv Drug Del Rev* 1998;29:39–49.
- [16] Osaka G, Carey K, Cuthbertson A, et al. Pharmacokinetics, tissue distribution, and expression efficiency of plasmid [³³P]DNA following intravenous administration of DNA/cationic lipid complexes in mice: use of a novel radionuclide approach. *J Pharm Sci* 1996;85:612–8.
- [17] Thorne RG, Emory CR, Ala TA, Frey WH. Quantitative analysis of the olfactory pathway for drug delivery to the brain. *Brain Res* 1995;692:278–82.
- [18] Mathison S, Nagilla R, Kompella UB. Nasal route for direct delivery of solutes to the central nervous system: fact or fiction? *J Drug Target* 1998;5:415–41.
- [19] Metzler B, Anderton SM, Manickasingham SP, Wraith DC. Kinetics of peptide uptake and tissue distribution following a single intranasal dose of peptide. *Immunol Invest* 2000;29:61–70.